Received 12 July 2022, accepted 15 August 2022, date of publication 23 August 2022, date of current version 31 August 2022.

Digital Object Identifier 10.1109/ACCESS.2022.3201136

RESEARCH ARTICLE

A Novel Dynamic Load Modeling for Power Systems Restoration: An Experimental Validation on Active Distribution Networks

ROBERTO BENATO[1], (Senior Member, IEEE), SEBASTIAN DAMBONE SESSA[1], (Member, IEEE), GIORGIO M. GIANNUZZI[2], COSIMO PISANI[2], MICHELE POLI[2], AND FRANCESCO SANNITI[1], (Member, IEEE)

[1]Department of Industrial Engineering, University of Padova, 35131 Padua, Italy
[2]Dispatching and Switching Department, Terna, 00156 Rome, Italy

Corresponding author: Sebastian Dambone Sessa (sebastian.dambonesessa@unipd.it)

This work was supported by the Terna through the "Consorzio Interuniversitario Nazionale Energia e Sistemi Elettrici" (ENSIEL) under Grant ST-196.

ABSTRACT In this paper, a novel approach to assess the power demand of distribution networks during a restoration process following an outage is presented. The possibility of correctly estimating such power demand represents a very important support in the choice and management of reliable restoration paths which significantly contributes to increase the resilience of the power system. In fact, due to the ever-growing penetration of renewable energy sources in the worldwide networks, electrical systems are often pushed to operate closer to their design limits and so, in particular conditions, black outs can be more frequent compared to the past. In this context, the aim of this work is to develop a general expression which can consider and represent all the key elements which affect the active and reactive power demand of distribution grids during the restoration process. The proposed method considers also the relationship between distributed generation and frequency behaviour in the power demand estimation. This aspect is generally neglected in literature although it has a significative impact. The effectiveness of the present approach is experimentally demonstrated on field. More specifically, the developed tool is applied to estimate the power demand of two real distribution networks and the tool results are compared with on-field recordings. This comparison demonstrates that the proposed approach represents a promising tool which, together with the restoration tests, could be an important ally in the design and management of the restoration plan of electrical networks.

INDEX TERMS Load modelling, cold load pick up, black start, power system restoration, modelling of distributed generation.

NOMENCLATURE

Symbol	Meaning
BS	Black Start.
c	p.u.l. line capacity [nF/km].
CLPU	Cold load pick up.
c_p	DG performance ratio.
DG	Distributed generation.
DN	Distribution network.
DSO	Distribution system operator.
ΔP_{DG1}	DG active power provided by PFR [W].
ΔP_{DG2}	DG active power provided by inertial response [W].
ΔP_{DL}	Load active power dynamic deviations [W].
ΔP_S	Load active power static deviations [W].
ΔQ_S	Load reactive power static deviation [VAr].
$f(t)$	Grid frequency [Hz].

The associate editor coordinating the review of this manuscript and approving it for publication was Gab-Su Seo.

f_n	Nominal grid frequency [Hz].
f_{min}, f_{max}	Min and max DG frequency threshold [Hz].
f_1, f_2, f_3, f_4	frequency limits for the activation of the PFR [Hz].
φ	Load power factor.
φ_{DG}	DG power factor.
GLME	General load modelling expression.
k_1	Max value for exponential rise [pu].
k_2	Max value for exponential decay [pu].
k_{rec}	Share of load recovery [pu].
$k_{1,2}$	Max value for exponential rise and decay [pu].
k_{pu}, k_{pf}, k_{qu}, k_{qf}	Exponents for load static deviations.
k_c	Current distribution coefficient.
l	p.u.l. line inductance [mH/km].
ℓ	Line length [km].
L2	Commercial load category.
L3	Artisan load category.
L4	Industrial load category.
LME	Load modelling equation.
LV	Low voltage.
MV	Medium voltage.
n_{DG}	Number of DG types.
OHL	Over head line.
P_{ss}	Load steady state power [W].
P_{inst}	DG nominal power [W].
P_{cont}	Load contractual power [W].
P_{peak}	Peak power of CLPU [W].
p_{peak}	Peak power of CLPU [pu].
p_{min}	Power when CLPU ends [pu].
P_{DG}^N	Active power of DG in nominal condition [W].
p_r	DG reconnection power ramp [pu/s].
P_{max}	maximum power deliverable by DG [W].
PFR	Primary frequency regulation.
P_J	Joule losses [W].
P_m	Active power on-field measurement [W].
$p.u.l.$	Per unit length.
Q_L	Reactive power exchanged by the load [VAr].
QLME	LME for the reactive power.
Q_{DG}	Reactive power provided by DG [VAr].
Q_L, Q_C	Inductive and capacitive reactive power exchanged by lines [VAr].
Q_m	Reactive power on-field measurement [VAr].
r	p.u.l. line resistance [mΩ /km].
σ_o	DG over-frequency droop.
σ_u	DG under-frequency droop.
τ_1	Time constant for exponential rise [s].
τ_2	Time constant for exponential decay [s].
t_0	DN re-supply instant [s].
t_1	CLPU rise time [s].
t_2	CLPU decay time [s].
T_a	Load start-up time [s].
T_N	DG start up time [s].
TN	Transmission network.
t_p	time at which p_{peak} occurs [s].
t_{rec}	Recovery time [s].
t_r	time at which p_{min} occurs [s].
t_{ss}	time at which p_{ss} is settled [s].
TSO	Transmission System Operator.
t_{ps}	DG reconnection time [s].
t_{out}	Outage time [s].
$u(t)$	Voltage at the point of connection [pu].
u_{min}, u_{max}	Min and max DG voltage threshold [pu].

I. INTRODUCTION

The identification of suitable restoration paths is a fundamental step to increase the resilience of electrical networks in order to deal with black out occurrences. In fact, due to the ever-growing penetration of renewable energy sources in the worldwide networks, electrical systems are often pushed to operate closer to their design limits and so, in particular conditions, black outs can be more frequent compared to the past.

Real restoration tests play a key role to verify the reliability of the network restoration plans because they make it possible to know not only the behaviour of the generators involved in the Black Start (BS), but also the active and reactive power absorbed by the electric load supplied by the restoration path as a function of both the grid frequency and voltage [1], [2], [3].

In this context, the possibility of having reliable tools to forecast the behaviour of the active and reactive power absorbed by the Distribution Network (DN) under a primary sub-station after an outage, significantly helps in the optimal setting of the restoration process. Moreover, although the distribution grid is traditionally considered as a passive electrical system, it is becoming more and more an active one. Hence, this aspect deserves to be considered in the power demand estimation of distribution grids. In technical literature, several efforts have been made to represent and to try to predict the load power demand of distribution networks during a re-energization.

A. LITERATURE REVIEW

Most of the authors concentrated their researches on the modelling and evaluation of the Cold Load Pick Up (CLPU). Based on this phenomenon, electric load aggregates characterized by a high penetration of thermostatically-controlled devices, in the first instants after a re-energization following an outage, absorb a power which is much higher than the one absorbed in the steady state condition [4], [5].

Hence, it is very important to be able to foresee the trend of the CLPU to correctly manage the restoration of DNs.

In [6], the authors described a measurement-based approach to evaluate the CLPU after an outage by means of an exponential formulation which is parametrized by exploiting experimental data.

This method is very useful and versatile to reproduce specific scenarios for which a set of measurement is available, but it cannot be considered a general approach to foresee the power demand of scenarios which are different from the parametrization ones.

In [7], the harmonic model theory to predict the CLPU of the load supplied by a given feeder after an outage is described. This approach is based on experimental measurements performed on a feeder to derive several parameters representing its power demand during the re-energization of the load. The method proven to be precise, but the needed parameters are many and they are specific for each feeder of a grid.

In [8], the Multi-State Load Models have been applied to foresee the CLPU on distribution feeders. The described approach is able to assess the CLPU magnitude and duration with high penetration of heat pumps but does not consider the possibility of having a mix of different load type categories.

In [9], [10], and [11], complex physical models to represent thermostatically-controlled loads are described. In particular, in [9], the information obtained regarding the thermal mass and thermal insulation of buildings together with meteorological data, is exploited to develop a thermic model to estimate the winter power demand of heating loads. In [10], a similar approach is used but a more simplified linear dynamic system model is applied, so to obtain a reasonable approximation of the heat flow which characterizes thermo-controlled loads. Such approaches are very detailed but they are tailored for only one load category and require parameters and data that may not always be available. In this regard, [11] highlights some negative effects that may occur when control parameters are not set properly by presenting a model capable of simulating the effect of various control parameters which affect the control strategy of water heater physical models.

In [12], an analytical procedure to assess the restoration of distribution systems is described, where the CLPU is represented by means of a delayed exponential model together with a thermodynamic model of the supplying transformer. The approach is interesting since it is completely analytical, but it is very simplified and it does not allow representing a mix of different load categories.

In [13], the load power demand of residential systems is modelled stochastically by using time-of-use curves published in several countries for research purposes. The model is not very detailed but, in this case, the aim of the model is to define reliability indices of residential loads including the CLPU rather than estimating in detail the power behaviour during the restoration process. In [14], an important issue is investigated, i.e. the time dependence of CLPU. A time dependent CLPU model is developed by analysing the operating state evolution of thermostatically controlled loads after an outage to characterize the time dependent behaviour of CLPU. The proposed method is very detailed but, from the other hand, is quite complex and it needs a numerical solution.

Another very important issue to consider in the modelling of the power demand of DNs during their restoration is the influence of the Distributed Generation (DG), which is more and more present nowadays due to the energy transition from fossil fuel to renewable energy sources.

From this standpoint, in [15] a model which considers both the CLPU effect and the DG plants disconnection as a function of the frequency is described. The contribution is valuable, but several aspects are neglected, such as the involving of DG in Primary Frequency Regulation (PFR) service and the possibility of having a mix of different load categories supplied by a DN.

In the power systems restoration field, also the study and development of innovative and effective load restoration algorithms represent an important area of research. In this context, the possibility of estimating the load power demand is an essential point and it is usually faced by applying numerical algorithms. In [16], the possibility of exploiting wind storage systems to support the restoration process is proposed, by presenting a numerical method which considers as input data the parameters of generating units, restored loads blocks, and their restoration time as well as the restored lines. The load power demand and in particular the CLPU effect are modelled by applying an exponential delayed model whose parameters are difficult to know for any scenario, especially in presence of a mix of load categories. Hence, it is difficult to apply such approach to foresee the power demand in a generic scenario. In [17], a heuristic technique based on breadth first-traversal search is employed in the determination of the switching sequence that leads the power grid to the restorative state. Although such method is able to indicate the best load restoration strategy, it does not propose a general method to estimate the power demand of DNs. In [18], a numerical method which indicates the formed de-energized islands and their loads after fault occurrence in the network is presented. This method can also check the radiality constraint of the network and evaluate the best load pickup sequence by considering the priorities of the loads, but it does not propose a general power demand estimation method.

B. CONTRIBUTION OF THE PAPER

Hence, from the literature review, it emerges that the restoration of DNs after an outage is widely investigated in the scientific community and faced by exploiting different approaches. The estimation of the absorbed power demand is a key point in this process and there is not an analytical procedure which is able to consider all the fundamental aspects which affect the behaviour of the power absorbed by a DN during its re-energization following an outage. Such key aspects are:

- the presence of a mix of different load categories;
- the presence of DG, by taking into account its behaviour as a function of time, voltage and frequency also

considering the PFR service together with the DG inertia;
- the static and dynamic behaviour of electric loads as a function of time, frequency and voltage;
- the power absorbed by the distribution lines.

The purpose of the research presented in this paper is the identification of a unique analytical and General Load Modelling Expression, (GLME in the following) to assess the power exchanged by DNs during their re-energization including the presence of DG during a restoration process. The necessary input parameters are relatively simple to identify and the procedural approach to derive them is presented. Despite the ease of use of the proposed formulation, all the variables of influence which affect the power demand behaviour as a function of the grid voltage and frequency are considered. Moreover, differently from the physical models described in literature, the proposed approach is able to correctly estimate the CLPU during the load restoration phase without the need of considering the physical variables which characterize the behaviour of thermostatically-controlled loads as an input. Hence, it needs a lower number of input variables.

Furthermore, in the estimation approaches described in literature, an analytical and complete description of the influence that the DG PFR service has in the power demand variations is missing, although it has a significative impact. Eventually, the proposed approach is completely general since it does not just work for a specific scenario, but it can be applied to any situation, as it is demonstrated in the reminder of the paper.

The developed procedure is experimentally validated by exploiting two on-field measurement campaigns carried out on two DNs characterized by different levels of DG penetration.

Tab. 1 summarizes the main pros and cons of the present GLME approach compared to other methods proposed in literature.

It is worth noting that the proposed method could be integrated in a distribution automation infrastructure. In fact, distribution automation approaches related to the restoration of power systems are investigated in technical literature.

In [19], a complete numerical tool for implementation and evaluation for fault location, isolation, and service restoration system for MV distribution network is presented. The result of this study shows how such method has a remarkable benefit observed by enhancing customers' satisfaction and reducing penalties from industry regulators. In [20], a heuristic service restoration algorithm is proposed in the form of a Bi-Stage algorithm that at the first stage quickly restore energy to some loads using remote controlled switches and in the second stage, all types of switches are used to complete the process. In [21], an integrated optimization model for unbalanced distribution system restoration after large-scale power outages caused by extreme events is presented. The model can coordinate the control actions of multiple types of distributed energy resources and also considers topology flexibility by forming dynamic islands through reconfiguration.

TABLE 1. Comparative table with pros and cons of GLME compared with other load modelling approaches.

	Physical models [8, 9, 10, 11, 12]	Measurement based models [6, 7, 15]	Restoration algorithms [16, 17, 18]	GLME
Small number of input data for power demand estimation	**no**	**yes**	**yes**	**yes**
Generality in the power demand estimation	**yes**	**no**	**no**	**yes**
DG PFR influence	**no**	**no**	**no**	**yes**
Automatic identification of the best restoration path	**no**	**no**	**yes**	**no**

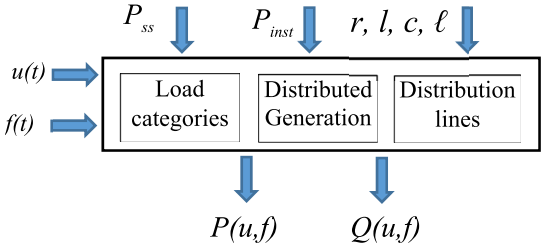

FIGURE 1. Logic scheme of the model.

II. METHOD

A. THE IDEA BEHIND THE MODEL

As summarized in Fig. 1, the considered input data for the model are:

- the steady state power P_{SS} absorbed by the loads, obtainable by starting from the load contractual power P_{cont} by applying a suitable utilization factor. It is worth noting that, in this context, the steady state power P_{SS} is meant as the power absorbed by the load if no contingencies are occurring in the Transmission Network (TN) which is supplying it.
- the frequency $f(t)$ and the voltage $u(t)$ of the network on the point of connection between the TN and the DN;
- the installed power P_{inst} of the DG subdivided according to the type of source, the power capacity and the voltage level of the point of connection;
- the resistance r, inductance l, capacitance c and length ℓ of the feeder lines (OHLs or Cables);
- The contractual power P_{cont} of the different load categories.

The electrical loads are divided in four main categories as follows:

- L1: residential electric loads related to residential energy contracts;
- L2: commercial electric loads related to commercial energy contract with a power consumption lower than 6 kW;
- L3: artisanal electric loads related to commercial energy contract with a power consumption between 6 kW and 100 kW;
- L4: industrial electric load related to commercial energy contract with a power consumption higher than 100 kW.

The L1 category is typically characterized by a strong presence of thermostatically-controlled loads.

In technical literature [4], [5], [6], [7], it is established that for such loads, in the first instants after a re-energization following an outage, the absorbed power is much higher than the power P_{SS} absorbed in the steady state condition, which is gradually reached after some time with a monotonically decreasing trend. This is the above mentioned CLPU phenomenon.

The categories from L2 to L4 behave differently compared to the L1 ones. In fact, from the technical literature [22] and from the experimental measurements shown in the reminder of this paper, it is possible to infer that for such load categories, following a re-energization, the absorbed power tends to be lower than the P_{SS} one, and then the steady-state condition is gradually reached in a given recovery time t_{rec}.

Hence, the peak power P_{peak} for these load categories can be considered equal to P_{SS}, i.e. $P_{peak\,L2-L4} = P_{SS}$.

Under these assumptions, a general equation called Load Modelling Equation (LME in the following), which is able to represent any electric load category at the nominal voltage and frequency, is developed. If the parameters of the LME are properly set, it is able to model the absorbed active power and the exchanged reactive one by any electric load aggregate. Moreover, the paper aims to provide a procedural approach to evaluate experimentally the parameters of the LME.

The LME is then combined with:

- an exponential approach to represent the static and the dynamic variations of electric loads as a function of voltage and frequency;
- the modelling of DG;
- the modelling of the line power losses.

The result of such combination is the GLME analytical expression to assess the power exchanged by DNs during their re-energization.

B. MODELLING OF THE LOADS IN NOMINAL CONDITIONS THOROUGH THE LME

The graphical representation of the LME in per unit is shown in Fig. 2. Let us assume that for $t = 0$ the DN is switched-off. At the time $t = t_0$ the network is re-energized and it is possible to note the presence of a power peak p_{peak} at the time t_p followed by an undershoot that brings the power at the value p_{min} and then, after the recovery time t_{rec}, the power reaches the p_{SS} value. Through this curve, it is possible to describe the active power absorbed by an electric load following a re-energization by identifying a general load trend containing the characteristic behaviours of all the electric load categories. In the time frame $t_1 + t_2$, such curve presents the characteristics of residential loads, and it can be represented as the joining of two exponential functions, characterized by the time constants τ_1 and τ_2.

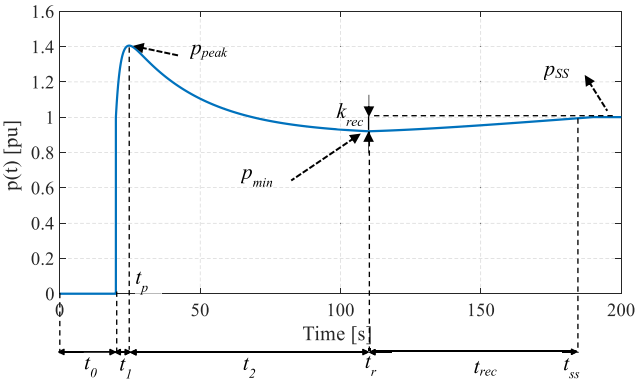

FIGURE 2. Graphical representation of the LME.

Hence, differently from the common approaches in literature, in this paper the CLPU effect is described by means of the sum of two exponential functions instead of a single exponential function. In the time frame from t_2 and t_{rec}, the curve can be described by exploiting an integral function which represents the characteristics of the load categories L2-L4.

Therefore, the power absorption described by the curve of Fig. 2 can be modelled by (1), in absolute values, for a given voltage and frequency (1), as shown at the bottom of the next page, where:

$$u_1(t) = H(t - t_0)$$

with, by referring to Fig. 2:

$u_1(t) = \mathrm{H}(t\text{-}t_0)$ the Heaviside function centred in t_0;

k_1 and k_2 are the maximum values of the two exponential functions;

$\tau_1 = t_1/ln(10)$ and $\tau_2 = t_2/ln(10)$;

$k_{rec} = p_{SS} - p_{min}$;

P_{ss} is active power in steady state in absolute value (MW);

$t_r = t_0 + t_1 + t_2$ and $t_{ss} = t_0 + t_1 + t_2 + t_{rec}$.

Since for $p(t_{ss}) = 1$, it yields that $k_2 = k_1 + k_{rec}$.

Since residential loads do not present a recovery time, for such category $k_{rec} = 0$ and consequently $k_2 = k_1 = k_{1,2}$. Regarding the load categories from L2 to L4, since it is assumed that $p_{peak\_L2-L4} = 1$, (1) can be rewritten, in steady state condition and in per unit, as (2):

$$1 + k_1(1 - e^{-(t-t_0)/\tau_1}) - k_2(1 - e^{-(t-t_0)/\tau_2}) + k_{rec} = 1 \tag{2}$$

where (2) is verified for $k_1 = 0$, $k_2 = k_{rec}$ and $\tau_1 = \tau_2 = 0$.

The parameter k_{rec} can assume different values depending on the type of industrial, artisanal, or commercial load category. Typical values of k_{rec} and t_{rec} are reported in [22]

based on the specific activity and on the type of industrial process.

The ranges of such values are:

- $0{,}6 < k_{rec} < 0{,}7$ and $300\text{s} < t_{rec} < 1000\text{s}$ for the L2 and L3 category;
- $0{,}6 < k_{rec} < 1$, e $3000\text{s} < t_{rec} < 10800\text{s}$ for the L4 category.

With regard to the parameter $k_{1,2}$, its value has to be assessed experimentally. It is possible to infer it by starting from the assumption that $k_{1,2}$, τ_1 and τ_2 have a narrow range of variation for residential loads. In other words, the shape of the CLPU is considered almost the same for the L1 load category, irrespective of the analysed scenario, with an acceptable margin of error. What changes is the magnitude of the phenomenon, which is related to the P_{SS} value as described by (1). The consistency of such assumption is experimentally demonstrated in the model validation section. Hence, by measuring the $P_{peak} = p_{peak} \cdot P_{ss}$ of a given residential load during its re-energization following an outage together with the times t_1+t_2, it is possible to deduce the value of $k_{1,2}$ and to apply (1) to represent any electric load.

In fact, the P_{peak} value is reached for the time t_p where the derivative of the two exponential functions is null, as described by (3) and (4)

$$\frac{d}{dt}\left[k_1(1-e^{-t_p/\tau_1})\right] = \frac{k_1}{\tau_1}e^{-t_p/\tau_1} = 0 \tag{3}$$

$$\frac{d}{dt}\left[k_2(1-e^{-t_p/\tau_2})\right] = \frac{k_2}{\tau_2}e^{-t_p/\tau_2} = 0 \tag{4}$$

The time t_p can be then expressed by means of (5):

$$t_p = \frac{\ln\left(\frac{k_2}{\tau_2}\right) - \ln\left(\frac{k_1}{\tau_1}\right)}{\frac{1}{\tau_2} - \frac{1}{\tau_1}} \tag{5}$$

By substituting (5) in (1) for $t = t_p$, and by posing $u_2(t) = 0$, it yields that $LME(t) = p(t) = p_{peak}$. Hence, (1) can be expressed in per unit by (6):

$$p_{peak} = 1 + k_1\left(1 - e^{-\frac{\ln\left(\frac{k_2}{\tau_2}\right)-\ln\left(\frac{k_1}{\tau_1}\right)}{\tau_1\left(\frac{1}{\tau_2}-\frac{1}{\tau_1}\right)}}\right) - k_2\left(1 - e^{-\frac{\ln\left(\frac{k_2}{\tau_2}\right)-\ln\left(\frac{k_1}{\tau_1}\right)}{\tau_2\left(\frac{1}{\tau_2}-\frac{1}{\tau_1}\right)}}\right) \tag{6}$$

By considering that $k_2 = k_1 = k_{1,2}$ for residential loads, (6) can be rewritten as in (7) with $k_{1,2}$ as the only unknown parameter. (7) can be solved numerically to obtain $k_{1,2}$.

In order to assess the active power absorption for several electric load categories supplied by the same feeder, (1) can be rewritten and applied as in (8), by properly setting the values of the coefficients based on the load category.

$$p_{peak} = k_{1,2}\left[1-\left(\frac{k_{1,2}}{\tau_2}\right)^{-\frac{1}{\tau_1\left(\frac{1}{\tau_2}-\frac{1}{\tau_1}\right)}}\left(\frac{k_{1,2}}{\tau_1}\right)^{-\frac{1}{\tau_1\left(\frac{1}{\tau_2}-\frac{1}{\tau_1}\right)}}\right] + -k_{1,2}\left[1-\left(\frac{k_{1,2}}{\tau_2}\right)^{-\frac{1}{\tau_2\left(\frac{1}{\tau_2}-\frac{1}{\tau_1}\right)}}\left(\frac{k_{1,2}}{\tau_1}\right)^{-\frac{1}{\tau_2\left(\frac{1}{\tau_2}-\frac{1}{\tau_1}\right)}}\right]+1 \tag{7}$$

$$LME^{tot}(t) = \sum_{i=1}^{4}(LME_{Li}) \tag{8}$$

Since the power factor φ_i of each load category assumes typical values which are quite simple to estimate by knowing the supplied load types, the reactive power $Q_L^{tot}(t)$ absorbed in nominal conditions can be computed by means of (9):

$$QLME^{tot}(t) = \sum_{i=1}^{4}(LME_{Li})\tan\varphi_{Li} = \sum_{i=1}^{4}(QLME_{Li}) \tag{9}$$

C. MODELLING OF THE DISTRIBUTED GENERATION

With the aim of modelling correctly the reconnection of the DG units to the DN, the following aspects are considered:

- The type of the DG source;
- The performance ratio for each DG source type;
- The operating time before a DG unit can start to supply power again once the voltage is restored on its connection bus;
- The power slope to restore the pre-contingency active power production;
- The participation of DG sources to the PFR;
- The variation of the power production as a function of the frequency fluctuations;
- The frequency and the voltage thresholds which determine the intervention of the network interface relays, by disconnecting the DG plants;

By taking into account the performance ratio c_{pk}, the total active power P_{DG}^{N} provided by DG sources in nominal

$$LME(t) = \begin{cases} P_{SS}\left(1 + k_1(1-e^{-(t-t_0)/\tau_1}) - k_2(1-e^{-(t-t_0)/\tau_2})\right)u_1(t) & \text{if } t_0 < t < (t_1+t_2) \\ P_{SS}\left[\left(1 + k_1(1-e^{-(t-t_0)/\tau_1}) - k_2(1-e^{-(t-t_0)/\tau_2})\right)u_1(t) + \int_{t_r}^{t-t_r}\frac{k_{rec}}{t_{rec}}dt\right] & \text{if } t_r < t < t_{ss} \\ P_{SS} & \text{if } t > t_{ss} \end{cases} \tag{1}$$

TABLE 2. Typical reconnection times and production ramps of different DG sources.

	Photovoltaic	Thermal	Wind	Hydro
t_{ps} [s]	20	600	20	600
p_r [pu (P_{inst})/sec]	0.5	0.0007	0.5	0.025

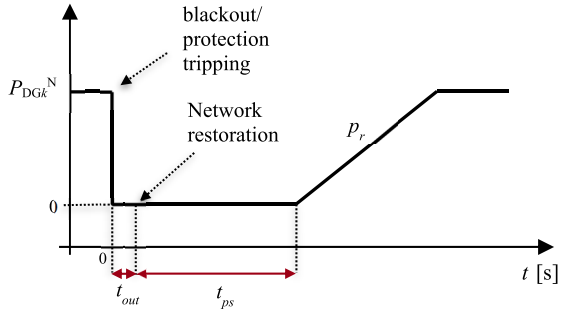

FIGURE 3. DG active power behaviour following a disconnection.

condition can be expressed as:

$$P_{DG}^{N} = \sum_{k=1}^{n_{DG}} P_{DGk}^{N} = \sum_{k=1}^{n_{DG}} c_{pk} P_{inst\_k} \tag{10}$$

where:

P_{inst_k} is the sum of the nominal power of each single installed DG unit of the source type k;

n_{DG} is the number of DG source types;

P_{DGk}^{N} is the active power provided by the k-th DG source in nominal condition.

The operating time before the reconnection depends on the DG source characteristics, on the prescriptions of the Grid Code and on the TSO requirements. In fact, the minimum reconnection time is needed to perform the start-up sequence and to prevent a sudden disconnection, but it could be higher based on the nation grid code prescriptions [23], [24], [25].

The typical reconnection times t_{ps} considered in this paper are reported in Table 2. The steady state power $P_{\mathrm{DG}k}^{\mathrm{N}}$ of each DG source is not reached instantaneously. A linear behaviour is assumed, as it is shown in Fig. 3. Table 2 reports the slopes of the curve based on the DG source type.

For the inverter-based generation, the starting times suggested by [26] are adopted, whereas for the rotating-machine based generation, they are set in accordance with the type of DG source [27].

With the aim of considering the participation of the DG to the PFR, it is necessary to model the variation of the power supplied by each DG source as a function of the network frequency. In this context, both the maximum action time of the frequency regulation and the regulation mode in case of underfrequency or over frequency are considered.

The DG frequency regulation mode can be described by (11) [26], [27].

$$\Delta P_{DG1k}(f,t) = \begin{cases} 0 & \text{if } f(t) < f_1 \text{ and} \\ & f_2 < f(t) < f_3 \\ P_{\max} \cdot \dfrac{f_2 - f(t)}{f_n \cdot \sigma_o} & \text{if } f_1 < f(t) < f_2 \\ \left(P_{\max} - \dfrac{f_2 - f_1}{f_n \cdot \sigma_u}\right) & \\ \quad \cdot \dfrac{f(t) - f_3}{f_n \cdot \sigma_o} & \text{if } f_3 < f(t) < f_4 \end{cases} \tag{11}$$

where:

ΔP_{DG1k} is the power contribution provided by the k-th DG source;

σ_o and σ_u are the droops in over-frequency and under-frequency respectively;

P_{max} is the maximum power deliverable by the DG source which differs respect to P_{DGk}^{N} because a certain amount of reserve power is considered, in order to perform the PFR;

$f_1, f_2, f_3 f_4$ are the frequency limits for the activation of the PFR;

f_n is the nominal frequency. Eq. (11) can be represented graphically as in Fig. 4. It is important to note that the DG power increase following the underfrequency has to be kept constant during the restoration of the nominal frequency, as represented by the red line in Fig. 4.

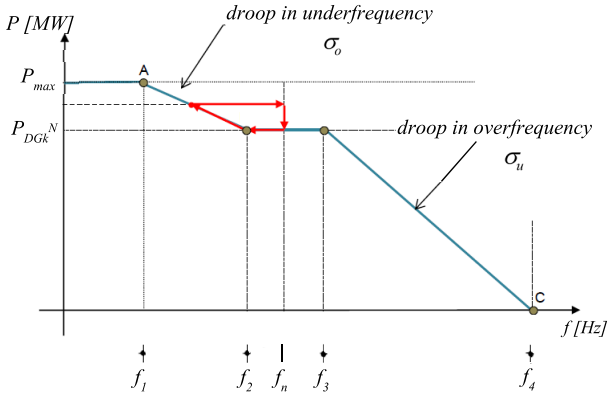

FIGURE 4. Power contribution of DG plants during the PFR service.

Regarding rotating DG generators, their inertial behaviour during the frequency fluctuations can be assessed by exploiting the concept of start-up time T_N of the generator, by means of (12) [28]:

$$\Delta P_{DG2k}(f,t) = \frac{P_{inst\_k} \cdot T_N}{f_n} \cdot \frac{d}{dt}\left(\frac{f_n - f(t)}{f_n}\right) \tag{12}$$

with f_n the nominal frequency.

Hence, by identifying the maximum and minimum voltages u_{max} and u_{min} and frequencies f_{max} and f_{min} for which the DG sources are disconnected, it is possible to consider the DG power contribution as a function of voltage and frequency

as in (13), as shown at the bottom of the page, where P_{GDk} is defined as in (14). The values of $u_{min}, u_{max}, f_{min}, f_{max}$ are different according to the type of source, its power capacity, the voltage level at the point of connection and the year of connection.

$$P_{DGk}(t) = \begin{cases} 0 & \text{if } t < t_0 + t_{ps} \\ P^N_{DGk} \cdot p_r \cdot (t - t_0 - t_{ps}) & \text{if } t_0 + t_{ps} < t < t_0 + t_{ps} + \dfrac{c_{pk}}{p_r} \\ P^N_{DGk} & \text{if } t > t_0 + t_{ps} + \dfrac{c_{pk}}{p_r} \end{cases} \tag{14}$$

As regards the reactive power control of each DG, the constant power factor mode is adopted, since it is one of the most widespread operation modes for the DG [23]. Therefore, the reactive power $Q_{DGk}\,(f, u)$ can be derived by knowing the power factor imposed for each DG source [24], [25] by means of (15).

$$Q_{DG}(t) = \sum_{k=1}^{n_{DG}} P_{DG_k}(t) \cdot \tan(\cos^{-1}(\cos \varphi_{DGk})) \tag{15}$$

D. STATIC AND DYNAMIC LOAD POWER VARIATIONS

In order to define a general expression describing the behaviour of electric loads, also the static and dynamic variations as a function of voltage and frequency have to be considered.

Regarding the static variation of the active power ΔPs_{Li} and the reactive one ΔQs_{Li} for the *i-th* load category, the exponential models described by (16) and (17) are considered [29]:

$$\Delta P_{SLi}(U, f) = LME_{Li}\left(\left(\frac{U(t)}{U_n}\right)^{k_{pu}}\left(\frac{f(t)}{f_n}\right)^{k_{pf}} - 1\right) \tag{16}$$

$$\Delta Q_{SLi}(U, f) = QLME_{Li}(t)\left(\left(\frac{U(t)}{U_n}\right)^{k_{qu}}\left(\frac{f(t)}{f_n}\right)^{k_{qf}} - 1\right) \tag{17}$$

where:

LME_i is obtained by (8)

$QLME_i$ is obtained by (9);

U_n is the nominal voltage;

$k_{pu}, k_{pf}, k_{qu}, k_{qf}$, are coefficients experimentally obtainable for each load category and also reported in literature [30].

The dynamic variations ΔP_{DLi} of the active power are related to rotating machines which change their power absorption based on the frequency of the network.

They can be assessed by means of (12), by applying the start-up time of the considered load category T_{aLi} instead of T_N. T_{aLi} can be assessed experimentally from load power measurement as a function of the network frequency variations by means of (18):

$$T_{aLi} = \frac{\Delta P \cdot f_n}{P_L \cdot \frac{\Delta f}{\Delta t}\Big|_{t_0}} \tag{18}$$

where ΔP is the power variation following the frequency variation Δf.

E. MODELLING OF THE LINE POWER LOSSES

In order to consider both the absorbed reactive power and power losses of the lines in the assessment of the power required by a DN during its re-energization, (19), (20), (21) and (22) can be applied for a given feeder j:

$$P_{J\_j} = \frac{r \cdot l_j}{U^2} \cdot k_C \left(\left(\sum_{i=1}^{4} (LME_{Li})_j - P_{GDj}\right)^2 + \left(\sum_{i=1}^{4} (QLME_{Li})_j - Q_{GDj}\right)^2\right) \tag{19}$$

$$Q_{L\_j} = \frac{2\pi f(t) \cdot \ell \cdot l_j}{U(t)^2} \cdot k_c \cdot \left(\left(\sum_{i=1}^{4} (LME_{Li})_j - P_{GDj}(t)\right)^2 + \left(\sum_{i=1}^{4} (QLME_{Li})_j - Q_{GDj}(t)\right)^2\right) \tag{20}$$

$$Q_{C\_j} = -U_n^2 2\pi f \cdot c \cdot l_j \left(\frac{U(t)}{U_n}\right)^2 \left(\frac{f(t)}{f_n}\right) \tag{21}$$

$$Q_{J\_j} = Q_{L\_j} - Q_{C\_j} \tag{22}$$

with

P_{J_j} the joule losses absorbed by the line j;

Q_{L_j} the inductive reactive power exchanged by the line j;

Q_{C_j} the capacitive reactive power exchanged by the line j;

ℓ_j the length of the line j;

r the kilometric resistance of the line;

$f(t)$ the instantaneous frequency;

$$P_{DG}(f, u) = \begin{cases} \sum_{k=1}^{n_{GD}} (P_{DGk} + \Delta P_{DG1k} + \Delta P_{DG2k}) & \text{if } u_{\min} < u < u_{\max} \text{and} \\ & f_{\min} < f < f_{\max} \\ 0 & \text{if } u < u_{\min} \text{ or } u > u_{\max} \text{ or} \\ & f < f_{\min} \text{ or } f > f_{\max} \end{cases} \tag{13}$$

l the kilometric inductance of the line;
c the kilometric capacitance of the line.

In this context, it is also necessary to define which is the distribution of the load and of the DG along the line and, consequently, to define the current distribution.

To this purpose, the coefficient k_c is introduced. The load and the DG are supposed uniformly distributed along the line, so that $k_c = 0{,}5$ whereas a unique concentrated load would imply $k_c = 1$, as it is shown in Fig. 5.

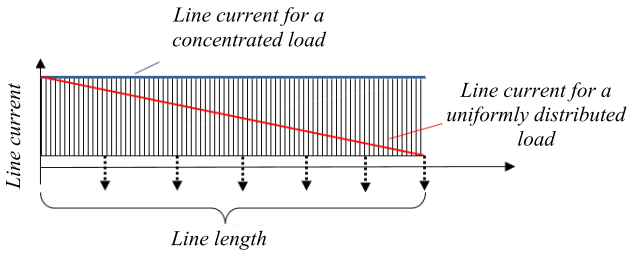

FIGURE 5. Meaning of the kc coefficient.

F. GENERAL EXPRESSION TO ASSESS THE POWER DEMAND DURING THE RESTORATION OF A DISTRIBUTION NETWORK

By combining the above-described equations to model the electric loads, the DG and the distribution lines, it is possible to identify the GLME to compute the active power absorbed by a DN with n feeders as a function of time, voltage and frequency in the form of (23).

Analogously, a similar expression to assess the exchanged reactive power can be written in the form of (24).

$$P(t) = \sum_{j=1}^{n} \left(\sum_{i=1}^{4} (LME_{Li} + \Delta P_{SLi} + \Delta P_{DLi})_j - P_{GDj} + P_{J\_j} \right) \quad (23)$$

$$Q(t) = \sum_{j=1}^{n} \left(\sum_{i=1}^{4} (QLME_{Li} + \Delta Q_{SLi})_j - Q_{GDj} + Q_{J\_j} \right) \quad (24)$$

The possibility of having a general expression which consider all the power contributions which affect the power demand of a DN after an outage, could represent a powerful and versatile tool in the power system management. The procedural approach to identify the unknown parameters of the described formulations together with their experimental validation are expounded in the following.

G. FIELD MEASUREMENTS CARRIED OUT ON REAL DNs TO PARAMETRIZE THE MODEL

In order to identify the coefficients of (7), the data related to the active power measured at the sending-end of two feeders (A and B) of two real DNs (1 and 2) of the Italian network are exploited, as it is shown in the scheme of Fig. 6.

The on-field measurements are performed during a real power system restoration test carried out by the Italian TSO Terna. During this test the DNs 1 and 2 were totally disconnected from transmission grid and then they were re-supplied. Fig 7 (blue curve) and Fig. 8 (blue curve) show the active power measurements P_{m_1} and P_{m_2} in the points A and B respectively during the re-supplying process. The optimal measurement situation in this context should be to identify lines devoted to supply only one load category but, in practice, this might not be possible. In fact, the measurement point indicated with A in Fig. 6 is related to a line which supplies a load composed of 78% L1, 21% L3 and 1% L4 together with a certain quantity of DG.

Hence, with the aim of obtaining the parameters $k_{1,2}$, τ_1, τ_2 for the L1 category, it is necessary to subtract from the power measurement the contributions of the DG, the line power losses and of the load categories from L2 to L4.

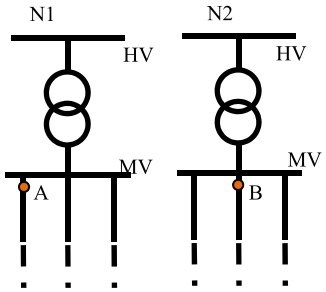

FIGURE 6. Points of measurement on the grid schemes for the model parametrization (grids highlighted in blue) and for the model validation (grids highlighted in green).

In Fig. 7, the CLPU effect is clearly visible since most of the loads belongs to the L1 category, and it is possible to see that the sum of two exponential functions represents its shape better than a single exponential one. This experimental evidence can be noted also in the CLPU measurements reported in literature [7], [8]. For this reason, in the above described CLPU modelling procedure the sum of two exponential functions is adopted instead of the commonly used single exponential function. The measurement point B in Fig. 6 is related to a cable line supplying a pure industrial load. From Fig. 8, it is possible to note how industrial load categories do not present the CLPU.

This evidence can be noted also in measurements reported in literature [22], and so (2) is confirmed.

H. SUBTRACTING THE DISTRIBUTED GENERATION POWER CONTRIBUTION

At first, the DG contribution has to be subtracted by the measured active power by exploiting (13), starting from the data of the DG installed power related to the feeder A and by applying suitable performance ratios. The yellow line in Fig. 7 represents the DG active power contribution computed by means of (13), by considering the prescription of the Italian grid code.

I. SUBTRACTING THE LINE POWER LOSSES

Once the DG contribution is subtracted from the measured power, the line power losses can be computed by

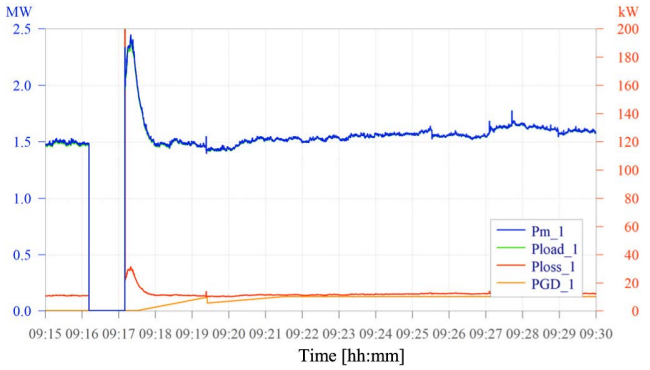

FIGURE 7. Measured active power through the point A of N1 and splitting in different elements.

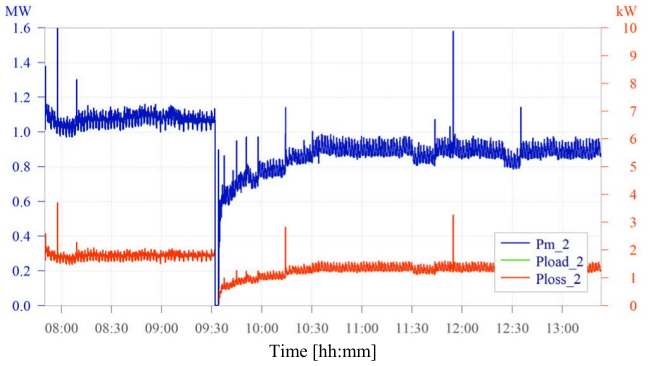

FIGURE 8. Measured active power through the point B of N2 and splitting in different elements.

applying (18), by substituting the measured active power P_{m_1} and the measured reactive one Q_{m_1}(not shown in the paper for the sake of brevity), and considering $P_{DG} = 0$, as it follows:

$$P(t)_{loss} = r \cdot \ell \cdot k_c \left(\frac{P_{m\_1}(t)^2 + Q_{m\_1}(t)^2}{U(t)^2} \right) \tag{25}$$

The red lines in Fig. 7 and Fig. 8 represent the power losses computed by means of (25).

J. INFERRING THE PARAMETERS $k_{1,2}$, τ_1, τ_2, t_{rec} AND k_{rec}

The green line in Fig. 8 represents the power measurements stripped of the power losses and of the DG contributions by exploiting (13) and (24), so having only the power P_{load_1} absorbed by the electric loads of the network 1. In this specific case, the green line is almost overlapped with the blue one (i.e. the measured power) due to the fact that the DG installed power in the considered DN is significantly less compared to the one of electric loads. However, the above described procedure is general and applicable especially to measurements carried out in electrical grids characterized by a high penetration of DG (as it is shown in the following). From the green line of Fig. 7 the value of the peak power P_{peak_L1} of the L1 category has to be obtained, by subtracting the contributions of the L3 and L4 load types. This is necessary because the power measurement of Fig. 7 is related to a mix of load categories comprising the load types L1, L3 and L4.

It is possible to assume that power absorbed by the L3 and L4 load categories is still at the initial value for the time t_p because of the loads L3 and L4 have a slower dynamic compared to the L1 one [22]. Therefore, P_{peak_L1} can be assessed by means of (26):

$$P_{peak\_L1} = P_{peak\_mix} - (1 - k_{rec\_L3}) \times P_{SS\_L3} - (1 - k_{rec\_L4}) P_{SS\_L4} \tag{26}$$

Hence, this procedural approach to parametrize the model is general and applicable even for feeders supplying a mix of loads. For the estimation of t_{rec} and k_{rec} related to the L4 category, the measurement of Fig. 8 can be exploited.

It is possible to derive that $k_{rec} = 0{,}5$ and $t_{rec} = 3474$ s. Such measured values substantially confirm the ones reported in [22], which can be used as a reference for the L3 category.

Eventually, by knowing the time instants t_1 and t_2 highlighted in Fig. 7, also the time constants τ_1 and τ_2 can be computed and (7) can be numerically solved in order to infer the parameter $k_{1,2}$. Table 3 reports the value experimentally obtained by applying the above described procedure.

TABLE 3. Parameters $k_{1,2}$, τ_1, τ_2 experimentally obtained.

Category	P_{peak_L1} [kW]	$k_{1,2}$	τ_1 [s]	τ_2 [s]
L1	2100.59	2.783	4.34	17.373

K. INFERRING THE START-UP TIME OF LOADS

In order to give an example of the assessment of the load start-up times, Fig. 9 shows the green line of Fig. 8, i.e. the measured power of the L1 category, as a function of the frequency variations. Eq. (17) is applied for different power variations and the average of the computed start-up times is considered as a final value. Table 4 shows an example of such procedure for two power variations. At the end of the procedure, $T_a = 0.44$ is obtained.

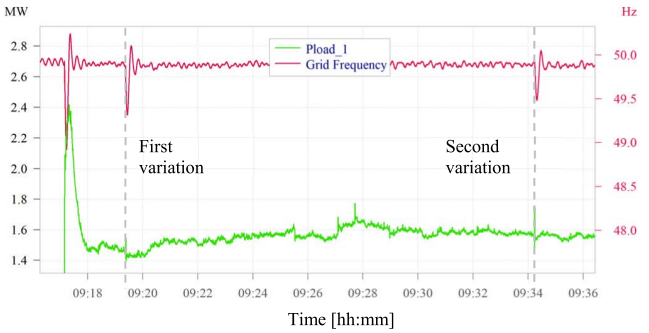

FIGURE 9. L1 category absorbed active power as a function of the frequency.

L. CASE STUDIES

The validation of the model is performed by exploiting the experimental measurements carried by the Italian TSO, Terna, during two on-field power system restoration tests.

TABLE 4. L1 load start-up time assessment for two power variations.

	$t_{initial}$ [hh:mm:s]	t_{final} [hh:mm:s]	$f_{initial}$ [Hz]	f_{final} [Hz]	$\Delta f / \Delta t$ [Hz/s]	$P_{initial}$ [MW]	P_{final} [MW]	ΔP [MW]	T_a [s]
First variation	9:19:9.13	9:19:9.88	49.87	49.65	0.295	1.466	1.411	0.044	0.41
Second variation	9:34:1.98	9:34:1.34	49.77	49.90	0.216	1.528	1.573	0.055	0.45

In the following, the two restoration tests, namely test *a*) and test *b*), are briefly described. The test *a*) was performed on a portion of the TN as represented in Fig. 10, which was temporary isolated from the rest of the network.

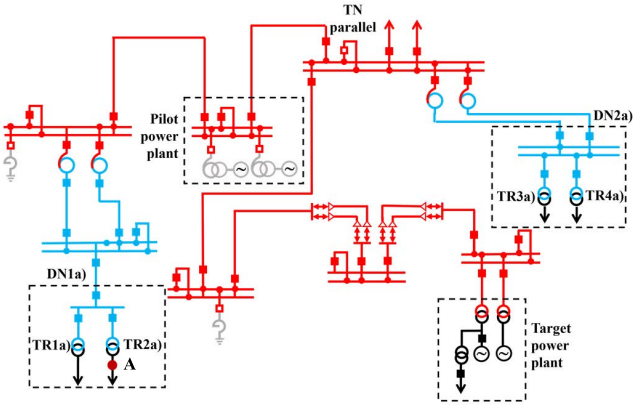

FIGURE 10. Single-phase representation of the TN portion involved in the restoration test a).

Red lines of Fig. 10 represent the 400 kV TN components, whereas the blue and black lines represent the 132 kV and 20 kV ones respectively.

The steps of the on-field restoration test *a*) can be summarized as follows:

- BS of the pilot power plant;
- Energization of the restoration path from the pilot power plant to the DN1a);
- Energization of the restoration path from the pilot power plant to the DN2a);
- Re-supply of DN1a);
- Re-supply of DN2a);
- Electric parallel between the restoration path and the target power plant;
- Electric parallel between the restoration path and the rest of the TN.

The point A in Fig. 10 indicates where the voltage, the frequency, the active and the reactive power were measured during the test.

The blue lines in Fig. 13 are the measured active and reactive power.

The contractual power P_{cont} under the feeders supplied by the MV busbar of TR1a), together with the length of the lines and the amount of DG are reported in Table 5.

TABLE 5. Data related to the feeders supplied by TR2a).

FEEDER	$P_{cont\ L1}$ [kW]	$P_{cont\ L2}$ [kW]	$P_{cont\ L3}$ [kW]	$P_{cont\ L4}$ [kW]	Cable Length [km]	OHL Length [km]	DG [MW]
1	3491.88		2569.3	4572	9.4	0.53	0.34
2	6612.6		1694.4	120	3.2	0	0.43
3	2891		3158.2	5165	7.1	0	0.08
4	7050.9		1344	420	5.3	0	0.02
5	0		0	1733	2.4	0	0.0
6	1083		1563.6	5237.9	4.5	0	0.03
7	7027.1		2078.15	200	5.3	0	0.17
8	9798.7		5013.68	2204	7.9	0.2	0.82
9	7721.44		2786.3	293	11.2	0	0.09
10	99		915.3	1388	3.5	0.6	0.15

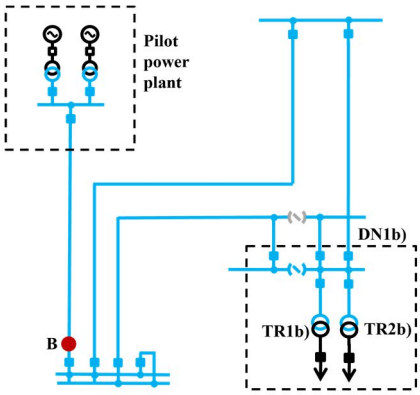

FIGURE 11. Single-phase representation of the TN portion involved in the restoration test b).

It is worth noting that for this test all the MV feeders are supplied simultaneously, by a single switching closure. It is possible to note how such a network is characterized by a modest amount of DG compared to the to load installed power.

The test *b*) was performed on the portion of the TN shown in Fig. 11.

The line colours of Fig. 11 have the same meaning of the ones of Fig. 10. The steps of the on-field restoration test *b*) can be summarized as follows:

- BS of the pilot power plant;
- Energization of the restoration path from the pilot power plant to the DN1b);
- Re-supply of DN1b);
- Electric parallel between the restoration path and the rest of the TN.

The point B in Fig. 11 indicates where the voltage, the frequency, the active and the reactive power were measured during the test.

The blue lines in Fig. 14 are the measured active and reactive power. The contractual power P_{cont} of the feeders

TABLE 6. Data related to the feeders supplied by TR1b) and TR2b).

FEEDER	$P_{cont\ L1}$ [kW]	$P_{cont\ L2}$ [kW]	$P_{cont\ L3}$ [kW]	$P_{cont\ L4}$ [kW]	Cable Length [km]	OHL Length [km]	DG [MW]
1	1164	123.5	543.6	357	7.3	6.2	0.41
2	71	39	235	625	7.3	6.2	0.097
3	0	0	0	1138	0.32	0	0
4	1791.5	168	770	580	0.82	0	0.28
5	2347.5	159.5	1916	500	4.19	0	0.59
6	922	121.15	1129	603	7.33	0	0.59
7	557.5	69.51	813	1072	12.2	16.7	0.52
8	157	30	90	0	12.2	16.7	0.03
9	2662.5	430,5	2019	655	1.8	16.5	1,1
10	3195	480	1493	270	10.82	0	0.63
11	663	185	939	750	5.048	0	0.345

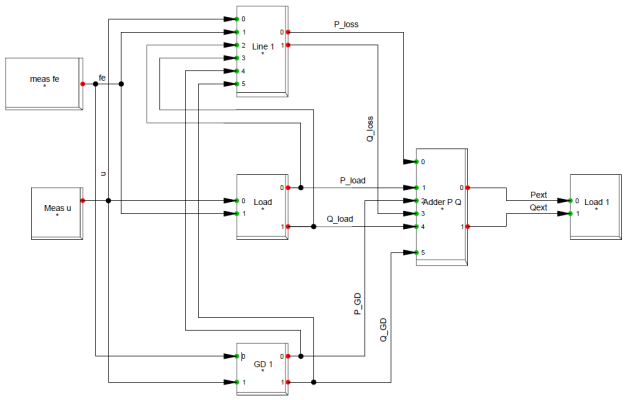

FIGURE 12. DIgSILENT implementation of the GLME for a single feeder.

supplied by TR1b) and TR2b), together with the length of the lines and the amount of DG are reported in Table 6. Differently from the previous DN, this one is characterized by a high penetration of DG with respect to the electric load installed power. In this case, differently from the test *a*), the feeders under TR1b) and TR2b) are supplied step-by-step.

It is worth noting that such DNs are different from the one on which the model is parametrized. This issue is extremely important in the model validation context since it demonstrates the effectiveness of the model itself. Of course, a validation performed on the same DN exploited for the parametrization process is useless since it obviously matches with the measurement records.

III. RESULTS AND DISCUSSION

In order to verify the effectiveness and the accuracy of the model presented in Sections III, the on-field measurements carried out on the case studies described in Section IV are compared with the output of the model. The data reported in Table 4 and Table 5 serve as input for the model, together with the voltage and frequency recorded during the two tests.

It is worth noting that all these data are related to the real DNs and have been collected in coordination with the Italian TSO and DSO. For this case study, the model is implemented in the DIgSILENT environment and Fig.12 shows the basic structure of it for a single feeder. It is worth noting that the voltage and the frequency inputs of the model are those measured at point A and B during the on-field restoration tests *a*) and *b*).

Fig. 13 shows the results of the comparison between the power measured on the point A during the restoration test *a*) and the output of the model.

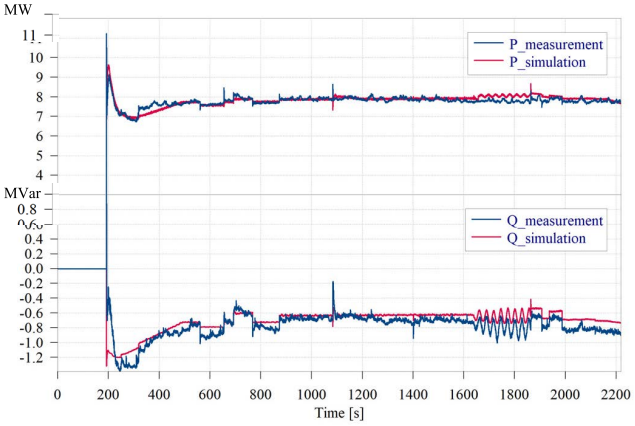

FIGURE 13. Comparison between the active power measured on the point A of DN1a) and the GLME response (upper figure) and the reactive power measured on the point A of DN1a) and the GLME response (bottom figure).

As shown in Fig. 13, by means of the correct parametrization procedure, the GLME is able to correctly identify the peak power required by the electric loads due to the CLPU phenomenon and also its dynamic.

Moreover, the active and reactive power variations as a function of the voltage and frequency are correctly assessed. Hence, even for DNs which are different with respect to the ones where the modelling equation is parametrized, this approach proven to be effective.

Fig. 14 shows the results of the comparison between the power measured on the point B during the restoration test *b*) and the output of the model.

From Fig. 14, the effect of the high penetration of DG in the DN is clearly visible. More specifically, after the re-connection of each feeder, the combination of two events influences the power behaviour. From one hand, the active power which transits through the point B decreases since the DG gradually supply the loads.

On the other hand, the frequency deviations following each step trigger the under-frequency relays of the DG units.

From both Fig. 13 and Fig. 14, it is possible to note that the DNs feature a resistive-capacitive behaviour, contrary to the expected. The proposed model correctly forecasts such behaviour due to the presence of the Cable line model. The ever-increasing penetration of cable installations on MV and LV side is thus the explanation of such unexpected behaviour.

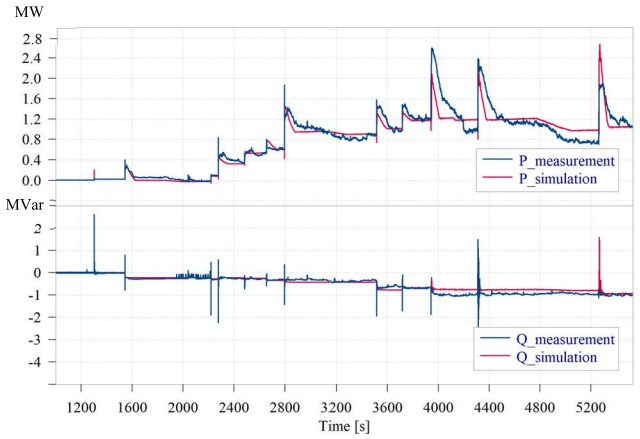

FIGURE 14. Comparison between the active power measured on the point B and the GLME response (upper figure) and the reactive power measured on the point B and the GLME response (bottom figure).

A. SIMPLIFYING ASSUMPTIONS APPLIED TO THE MODEL

In this section, the simplifying assumptions applied to the model are discussed. The first assumption deals with the utilization factors which are considered with a narrow range of variation for each load category. It is likely that such factors can be further refined by deriving them not only for load typologies, but also for the times of the year.

A second important consideration is that, in the model, it assumed that all the DG units perfectly comply with the grid code prescriptions regarding the protection settings. This might be not always verified in the complexity of the real network.

Another assumption is that the load categories from L2 to L4 behave in the same way after the re-energization. This behaviour has been inferred from literature [22]. However, if more data were available, it would be possible to better represent such load categories by refining the coefficients $k_{1,2}$, τ_1, τ_2, t_{rec}, k_{rec}.

Moreover, the influence of the outage time on the load behaviour has not been considered. Further researches are ongoing to consider also this phenomenon by maintaining the same approach.

As it is possible to infer from Figs. 13 and 14 the agreement between on-filed measurement and simulation is good. Despite the simplifying hypotheses adopted in the present paper, the comparison between predictive simulations and on field recordings on scenarios which are different from the ones adopted in the parametrization phase are promising.

The gap between measurements and simulation outputs can be allocated to the assumptions listed above.

The average percentage errors for the two tests are reported in Table 7.

Errors up to 19% might suggest a low precision of the present modelling approach, but it is necessary to highlight the challenging target of this study compared to the relative simplicity of the method. In particular, the higher displacement between the simulated power behaviour and the measured one is due to the lack of retrofit by some DG units regarding the frequency protection setting prescriptions.

TABLE 7. Percentage average errors on active and reactive power.

	Active power average error [%]	Reactive power average error [%]
test a)	1,6	11,2
test b)	12,6	19,2

As already mentioned, a higher data availability should improve the parametrization process and refine the displacements. This kind of approach is in tune with the ever-increasing availability of data in the DNs by means of the presence of smart meters.

IV. CONCLUSION

In this paper, a general procedural approach to foresee the power demand of a distribution network during a restoration process is presented and experimentally validated. The comparison between the on-field measurements and simulation results performed in two different distribution networks is encouraging. The adopted simplifying hypotheses are discussed in detail so that who wants to apply this method can overcome them if more data are available. Hence, by combining the novel approach described in this paper with the big data philosophy, it is possible to foresee the electric load behaviour very precisely for an optimal black start assessment of power systems.

The good agreement between the simulation results and the experimental measurements demonstrates that it is possible to exploit a unique and general expression to correctly foresee the active and reactive power demand of electrical networks as a function of the grid voltage and frequency. Moreover, the presented results also highlight that the cold load pick up phenomenon can be correctly assessed by properly parametrizing the load modelling equation. This avoids the implementation of physical models which require several input parameters that could be unknown, so that the presented approach overcomes the limitations of such physical methods. As it is described in detail in the paper, the presented method requires an initial parametrization starting from measurement data. In this regard, it is worth noting how the proposed formulation overcomes the main limitations of the measurement-based approaches, since it works not only for the specific scenarios where the model has been parametrized, but for any scenario, as demonstrated by the experimental validation of the method. Moreover, the analytical description of the dynamics based on which the distributed generation affects the power demand variation, allows estimating the power demand of both active and passive distribution networks. In particular, the analysed scenario characterized by a high penetration of distributed generation clearly shows how the frequency deviations following each restoration step trigger the under-frequency relays of the distributed generation units, by significantly influencing the active and reactive

power behaviour as a function of the grid voltage and frequency.

From the other hand, a limitation of the described approach is that in order to identify an optimal restoration path, it should be applied time after time since it is able to estimate the power demand of a specific distribution network. However, by combining the proposed estimation tool with black-start mock drills on the electrical network, it is possible to have a simple and very versatile tool to verify the performances of a chosen restoration path in order to increase the resilience of the electrical networks. Moreover, the proposed formulation could be combined with algorithms related to the automation distribution system approach, in order to try to make their structure easier and to reduce the computational burden of numerical algorithms. It is worth noting that the influence of the outage time on the load behaviour has not been considered in the CLPU estimation. Researches are ongoing to try to consider the CLPU outage time dependence by maintaining, on the same time, an analytical approach to estimate the power demand of distribution networks. This could increase the accuracy of the method.

REFERENCES

[1] R. Benato, G. Bruno, S. D. Sessa, G. M. Giannuzzi, L. Ortolano, G. Pedrazzoli, M. Poli, F. Sanniti, and R. Zaottini, "A novel modeling for assessing frequency behavior during a hydro-to-thermal plant black start restoration test," *IEEE Access*, vol. 7, pp. 47317–47328, 2019.

[2] K. Yamashita, J. Li, P. Zhang, and C.-C. Liu, "Analysis and control of major blackout events," in *Proc. IEEE/PES Power Syst. Conf. Exposit.*, Seattle, WA, USA, Mar. 2009, pp. 1–4.

[3] B. Li and P. Gomes, "Lessons learnt from recent emergencies and blackout incidents," Cigré Work. Group C2.21, Cigre Tech. Brochure 608, 2015.

[4] J. E. McDonald and A. M. Bruning, "Cold load pickup," *IEEE Trans. Power App. Syst.*, vol. PAS-98, no. 4, pp. 1384–1386, Jul. 1979.

[5] E. Agneholm and J. Daalder, "Cold load pickup of residential load," *IEE Proc.-Gener., Transmiss. Distrib.*, vol. 147, no. 1, pp. 44–50, Jan. 2000.

[6] C. Hachmann, G. Lammert, L. Hamann, and M. Braun, "Cold load pickup model parameters based on measurements in distribution systems," *IET Gener., Transmiss. Distrib.*, vol. 13, no. 23, pp. 5387–5395, 2018.

[7] J. Law, D. Minford, L. Elliott, and M. Storms, "Measured and predicted cold load pick up and feeder parameter determination using the harmonic model algorithm," *IEEE Trans. Power Syst.*, vol. 10, no. 4, pp. 1756–1764, Nov. 1995.

[8] K. P. Schneider, E. Sortomme, S. S. Venkata, M. T. Miller, and L. Ponder, "Evaluating the magnitude and duration of cold load pick-up on residential distribution feeders using multi-state load models," *IEEE Trans. Power Syst.*, vol. 31, no. 5, pp. 3765–3774, Sep. 2016, doi: 10.1109/TPWRS.2015.2494882.

[9] M. H. Nehrir, P. S. Dolan, V. Gerez, and W. J. Jameson, "Development and validation of a physically-based computer model for predicting winter electric heating loads," *IEEE Trans. Power Syst.*, vol. 10, no. 1, pp. 266–272, Feb. 1995, doi: 10.1109/59.373949.

[10] S. Ihara and F. C. Schweppe, "Physically based modeling of cold load pickup," *IEEE Trans. Power App. Syst.*, vol. PAS-100, no. 9, pp. 4142–4150, Sep. 1981.

[11] J. C. V. Tonder and I. E. Lane, "A load model to support demand management decisions on domestic storage water heater control strategy," *IEEE Trans. Power Syst.*, vol. 11, no. 4, pp. 1844–1849, Nov. 1996, doi: 10.1109/59.544652.

[12] C. Ucak and A. Pahwa, "An analytical approach for step-by-step restoration of distribution systems following extended outages," *IEEE Trans. Power Del.*, vol. 9, no. 3, pp. 1717–1723, Jul. 1994, doi: 10.1109/61.311189.

[13] A. Al-Nujaimi, M. A. Abido, and M. Al-Muhaini, "Distribution power system reliability assessment considering cold load pickup events," *IEEE Trans. Power Syst.*, vol. 33, no. 4, pp. 4197–4206, Jul. 2018.

[14] M. Song, R. R. Nejad, and W. Sun, "Robust distribution system load restoration with time-dependent cold load pickup," *IEEE Trans. Power Syst.*, vol. 36, no. 4, pp. 3204–3215, Jul. 2021.

[15] G. Lammert, A. Klingmann, C. Hachmann, D. Lafferte, H. Becker, T. Paschedag, W. Heckmann, and M. Braun, "Modelling of active distribution networks for power system restoration studies," *IFAC-PapersOnLine*, vol. 51, no. 28, pp. 558–563, 2018.

[16] L. Sun, W. Liu, C. Y. Chung, M. Ding, and J. Ding, "Rolling optimization of transmission network recovery and load restoration considering hybrid wind-storage system and cold load pickup," *Int. J. Electr. Power Energy Syst.*, vol. 141, Oct. 2022, Art. no. 108168.

[17] J. B. Leite, R. A. V. Peralta, and J. R. S. Mantovani, "Restoration switching analysis in the integrated architecture for distribution network operation," *Electric Power Syst. Res.*, vol. 194, May 2021, Art. no. 107069.

[18] S. Ghasemi and J. Moshtagh, "Distribution system restoration after extreme events considering distributed generators and static energy storage systems with mobile energy storage systems dispatch in transportation systems," *Appl. Energy*, vol. 310, Mar. 2022, Art. no. 118507.

[19] M. R. Elkadeem, M. A. Alaam, and A. M. Azmy, "Improving performance of underground MV distribution networks using distribution automation system: A case study," *Ain Shams Eng. J.*, vol. 9, no. 4, pp. 469–481, Dec. 2018.

[20] Q. Asadi, A. Amini, H. Falaghi, and M. Ramezani, "A heuristic algorithm for effective service restoration toward distribution networks automation," in *Proc. 15th Int. Conf. Protection Automat. Power Syst. (IPAPS)*, Dec. 2020, pp. 19–24.

[21] Z. Ye, C. Chen, B. Chen, and K. Wu, "Resilient service restoration for unbalanced distribution systems with distributed energy resources by leveraging mobile generators," *IEEE Trans. Ind. Informat.*, vol. 17, no. 2, pp. 1386–1396, Feb. 2021.

[22] E. Agneholm and J. E. Daalder, "Load recovery in different industries following an outage," *IEE Proc.-Gener., Transmiss. Distrib.*, vol. 149, no. 1, pp. 76–82, 2002.

[23] *IEEE Standard for Interconnection and Interoperability of Distributed Energy Resources With Associated Electric Power Systems Interfaces*, IEEE Std 1547-2018 (Revision of IEEE Std 1547–2003), 2018, pp. 1–138.

[24] *Regola Tecnica Di Riferimento Per La Connessione Di Utenti Attivi E Passivi Alle Reti BT Delle Imprese Distributrici Di Energia Elettrica (CEI 0–21)*, CEI Commettee, Apr. 2019.

[25] *Regola Tecnica Di Riferimento Per La Connessione Di Utenti Attivi E Passivi Alle Reti AT E MT Delle Imprese Distributrici Di Energia Elettrica (CEI 0–16)*, IEC Commettee, Apr. 2019.

[26] *Distributed Generation Analysis Case Study 6: Investigation of Planned Islanding Performance of Rotating Machine-based DG Technologies*, Natural Resour. Canada, Canmet Energy, Varennes, QC, Canada, Mar. 2012.

[27] Q. Yang, T. Yang, and W. Li, *Smart Power Distribution Systems: Control, Communication, and Optimization*. New York, NY, USA: Academic, 2019.

[28] A. Paolucci, *Lezioni Di Trasmissione Dell'Eneriga Elettrica*. CLEUP, 1998.

[29] A. Arif, Z. Wang, J. Wang, B. Mather, H. Bashualdo, and D. Zhao, "Load modeling—A review," *IEEE Trans. Smart Grid*, vol. 9, no. 6, pp. 5986–5999, Nov. 2018.

[30] J. V. Milanović and J. Matevosiyan, "Modeling and aggregation of loads in flexible power networks," Cigré Work. Group C4.605, Cigré Tech. Brochure 566, 2014.

ROBERTO BENATO (Senior Member, IEEE) was born in Venezia, Italy, in 1970. He received the Dr.Ing. degree in electrical engineering from the University of Padova, in 1995, and the Ph.D. degree in power systems analysis, in 1999. In 2021, he was appointed as a Full Professor with the Department of Industrial Engineering, University of Padova. He is the author of 200 papers and four books, edited by Springer, Wolters Kluwer, and China Machine Press. He has been a member of six Cigré Working Groups (WGs), the Secretary of two Joint WGs, and a member of IEEE PES Substations Committee. In 2014, he has been a Nominated Member of IEC TC 120 "Electrical Energy Storage (EES) Systems" in the WG 4 "Environmental issues of EES systems." He is currently a Corresponding Member of Cigré WG B1.72 "Cable rating verification secondnd part." In 2018, he has been elevated to the grade of a CIGRÉ Distinguished Member. He is a member of Italian AEIT.

SEBASTIAN DAMBONE SESSA (Member, IEEE) was born in Venezia, Italy, in 1981. He received the Dr.Ing. degree in electrical engineering from the University of Padova, in 2010, and the Ph.D. degree in power systems analysis, in 2017. In 2017, he was appointed as a Research Associate with the Department of Industrial Engineering, University of Padova. His research interests include transmission line modeling, fault location algorithms, stationary electrochemical and hybrid energy storage, high voltage direct current installations, and power system management. He has been a member of the Cigré working groups B1.47, B1.45, and B1.56. He is a member of Italian AEIT.

GIORGIO M. GIANNUZZI received the degree in electrical engineering from the University of Rome. Until December 2000, he worked at ABB, where he was in-charge of network studies, protection and control applications, with special reference to RTU apparatus and data engineering issues. Since 2001, he has been working at Terna as an Expert in defence plans/systems, dynamic studies, protection, telecontrol, and substation automation. From 2004 to 2011, he coordinated the study, design, and activation of wide area defence system (including interruptible customers system) and wide area monitoring system. In addition, under his guidance, the main security energy management systems were designed and coded. He supervised the revision of main Italian grid code technical enclosures.

COSIMO PISANI was born in Benevento, Italy, in 1985. He received the M.Sc. degree (Hons.) in energy engineering from the University of Sannio, Benevento, in 2010, and the Ph.D. degree in electrical engineering from the University of Naples "Federico II," Naples, Italy, in 2014. From May 2014 to March 2016, he was a Research Fellow with the University of Sannio. Since March 2016, he has been with Terna. He is currently a Senior Power System Engineer with the Dispatching and Switching Department—Stability and Network Calculations. His research interests include the applications of dynamic stability of power systems, wide area monitoring and protection systems, high voltage direct current systems, and power system restoration.

MICHELE POLI was born in Trento, Italy, in 1974. He received the Dr.Ing. degree in electrical engineering from the University of Padova, in 2001. Since 2001, he has been working at Terna (Italian TSO), where he deals with the analysis of the electrical phenomena in the unearthed and earthed operated HV networks, the power system defense against anomalous operations, the grid services performed by distributed generation sources, the network black start plans and restoration tests, and the verification of the grid code application. He has been a member of WG C2.25.

FRANCESCO SANNITI (Member, IEEE) was born in Feltre, Italy, in 1994. He received the Dr.Ing. degree in electrical engineering from the University of Padova, in 2019, where he is currently pursuing the Ph.D. degree in industrial engineering with the Department of Industrial Engineering. His research interests include dynamic modeling of frequency-voltage control systems for power system restoration, cables and OHL sequence impedance calculation, extremely high-voltage–high-voltage transmission lines and advanced matricial techniques for static, and dynamic power system analysis. He is a Young Member of CIGRÉ and AEIT.